

^{17}O MAS and 3QMAS NMR Investigation of Crystalline V_2O_5 and Layered $\text{V}_2\text{O}_5 \cdot n\text{H}_2\text{O}$ Gels

Craig J. Fontenot,^{†,‡} Jerzy W. Wiench,[‡] Glenn L. Schrader,^{†,‡} and Marek Pruski^{*,‡}

Contribution from the Department of Chemical Engineering and Ames Laboratory – USDOE, Iowa State University, Ames, Iowa 50011

Received April 12, 2002

Abstract: The environments for oxygen sites in crystalline V_2O_5 and in layered vanadia gels produced via sol–gel synthesis have been investigated using ^{17}O MAS and 3QMAS NMR. For crystalline V_2O_5 , three structural oxygen sites were observed: $\text{V}=\text{O}$ (vanadyl), V_2O (doubly coordinated), and V_3O (triply coordinated). Line-shape parameters for these sites were determined from numerical simulations of the MAS spectra. For the vanadia gels at various stages of dehydration, assignments have been proposed for numerous vanadyl, doubly coordinated, and triply coordinated oxygen sites. In addition, by correlating the ^{17}O MAS and 3QMAS NMR, ^{51}V MAS NMR, and thermogravimetric analysis data, the coordination of water sites has been established. On the basis of these results, the gel structure and its evolution at various stages of hydration have been detailed. Upon rehydration of the layered gel, we observed a preferred site for initial water readsorption. The oxygen atoms of these readsorbed water molecules readily exchanged into all types of oxygen sites even at room temperature.

1. Introduction

Metal oxides are used as semiconductor components, as well as various types of catalysts and ceramics. In catalysis, the role of oxygen in reducible metal oxides is of great importance for hydrocarbon selective oxidation, as the reactive lattice oxygen species can directly participate in the reaction. Our group recently reported results for the selective oxidation of 1,3-butadiene over vanadia–molybdena oxide gels,¹ prepared via a peroxo sol–gel method.² These materials were active at relatively low temperatures (275 °C) and produced valuable products such as maleic anhydride, furan, crotonaldehyde, and 3,4-epoxy-1-butene.

Metal oxides are often utilized in a noncrystalline state, which can make their characterization challenging. However, numerous advances in solid-state NMR have enhanced the spectroscopic characterization of disordered materials, such as gels or glasses. Magic-angle spinning (MAS) and various RF driven manipulations of spins can be used to average the first-order interactions that broaden the observed line shapes (mainly chemical shift anisotropy (CSA) and the dipolar coupling). Examination of half-integer quadrupolar nuclei such as ^{17}O ($I = 5/2$) requires the use of more complex techniques,^{3–7} including multiple-

quantum magic angle spinning (MQMAS) NMR,^{6,7} so that second-order quadrupolar broadening can be eliminated and high-resolution (isotropic) spectra can be obtained. In addition to site resolution, the isotropic chemical shift and quadrupolar parameters such as the quadrupole coupling constant can be obtained using these techniques.^{7,8}

Although NMR measurements of oxygen are challenging because of the very low natural abundance of ^{17}O nuclei (<0.03%), many samples can be enriched and studied under appropriate conditions. The majority of solid-state ^{17}O NMR studies have focused on materials containing Si and/or Al.^{9–11} The only ^{17}O NMR investigation of vanadia gels published to date investigated gels formed by the acidification of metavanadate salt solutions,¹² which were different from those prepared for this study by the peroxo-method,² although the same species were present in solution at the time of gelation. These studies concluded that mobile polymeric chains of vanadate octahedra were formed as the gelation progressed and that hydrogen bonding occurred between these chains.¹² Several resonances in the ^{17}O MAS NMR spectrum of the wet gel were identified and assigned to $\text{V}=\text{O}$, $\text{V}-\text{O}-\text{V}$, $\text{V}-\text{OH}$, and one type of $\text{V}-\text{OH}_2$ site.

^{17}O NMR studies have reported the detection of OH groups in titania-based xerogels,¹³ selected metal oxides and hydroxides,¹⁴ and glasses,⁹ but there are few ^{17}O investigations of

* To whom correspondence should be addressed. E-mail: mpruski@iastate.edu.

[†] Department of Chemical Engineering.

[‡] Ames Laboratory – USDOE.

- (1) Schroeder, W.; Fontenot, C. J.; Schrader, G. L. *J. Catal.* **2001**, *203*, 382.
- (2) Fontenot, C. J.; Wiench, J. W.; Pruski, M.; Schrader, G. L. *J. Phys. Chem. B* **2000**, *104*, 11622.
- (3) Llor, A.; Virlet, J. *Chem. Phys. Lett.* **1988**, *152*, 248.
- (4) Chmelka, B. F.; Mueller, K. T.; Pines, A.; Stebbins, J.; Wu, Y.; Zwanziger, J. W. *Nature* **1989**, *339*, 42.
- (5) Mueller, K. T.; Sun, B. Q.; Chingas, G. C.; Zwanziger, J. W.; Terao, T.; Pines, A. *J. Magn. Reson.* **1990**, *86*, 470.
- (6) Frydman, L.; Harwood, J. S. *J. Am. Chem. Soc.* **1995**, *117*, 5367.

- (7) Medek, A.; Harwood, J. S.; Frydman, L. *J. Am. Chem. Soc.* **1995**, *117*, 12779.
- (8) Massiot, D.; Touzo, B.; Trumeau, D.; Coutures, J. P.; Virlet, J.; Florian, P.; Grandinetti, P. J. *Solid State Nucl. Magn. Reson.* **1996**, *6*, 73.
- (9) Xu, Z.; Maekawa, H.; Oglesby, J. V.; Stebbins, J. F. *J. Am. Chem. Soc.* **1998**, *120*, 9894.
- (10) Pingel, U.-T.; Amoureux, J.-P.; Anupold, T.; Bauer, F.; Ernst, H.; Fernandez, C.; Freude, D.; Samoson, A. *Chem. Phys. Lett.* **1998**, *294*, 345.
- (11) Zhao, P.; Neuhoff, P. S.; Stebbins, J. F. *Chem. Phys. Lett.* **2001**, *334*, 325.
- (12) Pozarnsky, G. A.; McCormick, A. V. *J. Mater. Chem.* **1994**, *4*, 1749.

chemisorbed water. The sites for water adsorption in catalysts are of particular interest because water addition to hydrocarbon feedstocks can significantly alter both the activity and the selectivity of metal oxide catalysts,^{15–17} including those prepared in our previous work from vanadia gels.¹ The structural role of water in V_2O_5 has been, however, investigated in several TPD,^{18,19} vibrational spectroscopy,^{20–23} X-ray diffraction (XRD),^{24,25} and computational^{23,26,27} studies. Various conformations of water in $V_2O_5 \cdot nH_2O$ were proposed for different hydration levels and gel preparation methods.^{20–25} On the basis of the XRD data, Legendre et al.^{24,25} have introduced a ribbon model for the gels, in which V_2O_5 planes form two-dimensional $100 \text{ \AA} \times 1000 \text{ \AA}$ sheets composed of $27 \text{ \AA} \times 3.6 \text{ \AA}$ ($a \times b$) cells, which are spaced by $c = 11.55 \text{ \AA}$ for $n = 1.6$ or by $c = 8.75 \text{ \AA}$ for $n = 0.6$. These authors suggested that the water molecules were responsible for a shift of 2.8 \AA between the cells along the c axis, although the accurate localization of water was not possible. More specific models of water coordination have been offered in the studies that used vibrational spectroscopy.^{21–23} Livage et al.^{21,22} proposed a single water molecule for $n = 0.5$ centered between two doubly coordinated and two triply coordinated oxygen sites in one layer and four vanadyl oxygen atoms in the adjacent layer. For $n = 1.8$, the structure involved one water molecule coordinated to a vanadium site and hydrogen bonded to a second water molecule, which, in turn, formed a hydrogen bond with a vanadyl oxygen from the adjacent layer. Again, the c values of 8.8 and 11.5 \AA were determined for $n = 0.5$ and 1.8 , respectively. A somewhat different structure was proposed by Repelin et al.,²³ which for $n = 0.3$ involved a single water molecule hydrogen bonded to two vanadyl oxygen atoms from the same layer. At $n = 0.6$, this water molecule was joined (via a hydrogen bond) with a second one, which was also axially coordinated to a vanadium atom in the adjacent layer. Two additional water molecules were postulated to intercalate between these sites when $n = 1.4$.

Oxygen exchange from water into solid-state sites has been previously reported for several oxides, although usually a large amount of thermal energy was required for the exchange to occur. For example, Cameron et al.²⁸ determined an exchange rate k on the order of $10^{-2}/\text{min}$ and $10^{-4}/\text{min}$ at $488 \text{ }^\circ\text{C}$ of ^{18}O in Alundum-supported $V_2O_5\text{-D}_2O$ and $V_2O_5\text{-O}_2\text{-D}_2O$ systems, respectively. The exchange of ^{18}O from adsorbed water into ZSM-5 was investigated by von Ballmoos.²⁹ Nearly all of

the oxygen sites were observed to exchange within 1 h under steaming conditions at $600 \text{ }^\circ\text{C}$. The water-induced cleavage of Si–O–Si and Si–O–Al bonds was thought to give rise to the formation of hydroxyl groups. The exchange of ^{18}O from adsorbed CO_2 into zeolite A and $\text{AlPO}_4\text{-5}$ was reported by Endoh et al.^{30,31} They concluded that the highly reactive oxygen sites in the zeolites were associated with defects or amorphous regions.

We have previously reported studies of the peroxo-based sol–gel synthesis of layered and nonlayered vanadia gels using ^{51}V liquid-state NMR and laser Raman spectroscopy.² Subsequent characterization of the hydrated gels used solid-state ^{51}V NMR and TGA to elucidate various vanadium sites and the structural role of water in these materials.³² In the current work, we employed ^{17}O MAS and MQMAS NMR, as well as line-shape simulation methods, to determine directly the coordination of oxygen in crystalline V_2O_5 and layered vanadia gels. The ^{17}O MAS and MQMAS NMR spectra of the gels studied were surprisingly complex. In addition to structural oxygen sites, a detailed model of water coordination in the hydrated gels is shown that is consistent with our earlier ^{51}V NMR data.³² Finally, the complete structure of layered $V_2O_5 \cdot nH_2O$ gels is presented for $0 \leq n \leq 2$. In addition, the role of readsorbed water was examined, and evidence was obtained for room-temperature oxygen exchange between water and many of the oxygen sites of the gel matrix. Although some of the proposed assignments are open to further consideration, the results of this study show that these ^{17}O methods can enormously enhance the analytical capabilities of solid-state NMR in the area of oxidation catalysis.

2. Experimental Section

2.1. Sample Preparation. Results are reported for two layered samples: sample **I** was prepared using ^{17}O -enriched water (40%, Isotec), whereas sample **II** was synthesized using standard deionized water. The synthesis method used for sample **II** has been identical to that reported previously:³² a peroxovanadate solution was prepared by addition of 10 mL of 30% H_2O_2 solution in water (Fisher Chemicals) to a slurry of 1.0 g of V_2O_5 (Alpha Aesar) in 100 mL of deionized water. As a result, a $n(\text{H}_2\text{O}_2)/n(\text{V})$ molar ratio of 7.9 was achieved. The temperature of the sample was maintained at $25 \text{ }^\circ\text{C}$ during gelation and drying. For the rehydration experiments, the sample was heated to $224 \text{ }^\circ\text{C}$, cooled to room temperature, and exposed to H_2^{17}O vapor for 2 days at $20 \text{ }^\circ\text{C}$, all under N_2 atmosphere.

The synthesis of sample **I** has been somewhat modified to minimize the dilution of ^{17}O nuclei in the gel and thereby to conserve ^{17}O -enriched water: 30% H_2O_2 solution in water was replaced by 50% solution (155 μL) and added to a slurry of 70 mg of V_2O_5 in 0.3 mL of ^{17}O -enriched water, which produced $n(\text{H}_2\text{O}_2)/n(\text{V})$ and $n(\text{H}_2^{17}\text{O})/n(\text{V})$ molar ratios of 3.5 and 8.2, respectively. The temperature of the sample was maintained at $2 \text{ }^\circ\text{C}$ during the synthesis and at $25 \text{ }^\circ\text{C}$ during drying.

2.2. Solid-State NMR Spectroscopy. Solid-state NMR spectra of ^{51}V and ^{17}O were obtained using a Chemagnetics Infinity spectrometer operated at 105.17 and 54.2 MHz, respectively. Samples were placed in 3.2 mm rotors and spun at 20 kHz (unless noted otherwise) in a Chemagnetics MAS probe. All of the experiments were performed at room temperature following transfer of the thermally treated samples

- (13) Blanchard, J.; Bonhomme, C.; Maquet, J.; Sanchez, C. *J. Mater. Chem.* **1998**, *8*, 985.
- (14) Walter, T.; Turner, G.; Oldfield, E. *J. Magn. Reson.* **1988**, *76*, 106.
- (15) Park, D.-W.; Kim, D.-U.; Woo, H.-C.; Cho, Y.-G. Abstracts of Papers, 222nd ACS National Meeting, August 26–30, Chicago, IL, 2001.
- (16) Hocevar, S.; Levec, J. Abstracts of Papers, 222nd ACS National Meeting, August 26–30, Chicago, IL, 2001.
- (17) Henrich, V. E. *Rep. Prog. Phys.* **1985**, *48*, 1481.
- (18) Ranea, V. A.; Vicente, J. L.; Mola, E. E.; Arnal, P.; Thomas, H.; Gambaro, L. *Surf. Sci.* **2000**, *463*, 115.
- (19) Moshfegh, A. Z.; Ignatiev, A. *Surf. Sci.* **1992**, *275*, L650.
- (20) Abello, L.; Husson, E.; Repelin, Y.; Lucazeau, G. *J. Solid State Chem.* **1985**, *56*, 379.
- (21) Livage, J. *Chem. Mater.* **1991**, *3*, 578.
- (22) Vandendorre, M. T.; Prost, R.; Huard, E.; Livage, J. *Mater. Res. Bull.* **1983**, *18*, 1133.
- (23) Repelin, Y.; Husson, E.; Abello, L.; Lucazeau, G. *Spectrochim. Acta, Part A* **1985**, *41*, 993.
- (24) Legendre, J. J.; Livage, J. *J. Colloid Sci.* **1983**, *94*, 75.
- (25) Legendre, J. J.; Aldebert, P.; Baffier, N.; Livage, J. *J. Colloid Sci.* **1983**, *94*, 84.
- (26) Ranea, V. A.; Vicente, J. L.; Mola, E. E.; Uyewa Mananu, R. *Surf. Sci.* **1999**, *442*, 498.
- (27) Yin, X.; Fahmi, A.; Han, H.; Endou, A.; Ammal, S. S. C.; Kubo, M.; Teraishi, K.; Miyamoto, A. *J. Phys. Chem. B* **1999**, *103*, 3218.
- (28) Cameron, W. C.; Farkas, A.; Litz, L. M. *J. Phys. Chem.* **1953**, *57*, 229.

- (29) von Ballmoos, R. *The ^{18}O -Exchange Method in Zeolite Chemistry*; Otto Salle Verlag: Frankfurt, 1981.
- (30) Endoh, A.; Mizoe, K.; Tsutsumi, K.; Takaishi, T. *J. Chem. Soc., Faraday Trans. 1* **1989**, *85*, 1327.
- (31) Takaishi, T.; Endoh, A. *J. Chem. Soc., Faraday Trans. 1* **1987**, *83*, 411.
- (32) Fontenot, C. J.; Wiench, J. W.; Pruski, M.; Schrader, G. L. *J. Phys. Chem. B* **2001**, *105*, 10496.

to the probe within a glovebox under dry N_2 . Shifts are reported using the δ scale, with positive values being downfield and referenced to $VOCl_3$ for ^{51}V NMR and water for ^{17}O NMR.

^{51}V MAS NMR spectra were obtained using the Hahn echo sequence ($\pi/2 - \tau - \pi - \tau$ - acquisition) and a high RF field of 100 kHz. Additional experiments performed at lower RF fields, with and without the use of an echo, ensured that no distortions were present in the reported spectra. Typically, 1000 scans were accumulated using a relaxation delay of 0.2 s.

For the ^{17}O MAS experiments, the Hahn echo pulse sequence was used, along with an extended 16-phase cycling, which was introduced to eliminate acoustic ringing.³³ A delay of 2 s between the scans was required to ensure complete relaxation for all resonances observed in these experiments. The triple-quantum MAS (3QMAS) experiments employed the standard z -filtered method³⁴ and were optimized using a sample of ^{17}O -enriched silica. The magnitudes of the RF fields used in these experiments were 104 and 5.6 kHz for nonselective and selective pulses, respectively. For 3QMAS experiments, a delay of 500 ms was sufficient for the sites being examined and thus was used to shorten the overall acquisition time. Still, because of the small concentration of ^{17}O nuclei and the limited overall efficiency of the 3QMAS experiment, acquisition times of up to 3 days were required.

Numerical simulations of the ^{17}O and ^{51}V MAS spectra of crystalline V_2O_5 were performed using QUASAR.³⁵ These simulations included the effects of the CSA as well as first- and second-order quadrupolar interactions; both central and satellite transitions were considered. Several line-shape parameters describing these interactions have been determined, including the quadrupole coupling constant (C_Q), the asymmetry parameter (η_Q), the isotropic chemical shift (δ_{iso}), the CSA ($\Delta\delta_{CSA}$), and the CSA asymmetry parameter (η_{CSA}). In addition, the isotropic chemical shifts were determined directly from the ^{17}O 3QMAS spectra.^{8,36}

2.3. Thermogravimetric Analysis. Samples were analyzed using a Perkin-Elmer TGA 7 instrument. Heating rates were 5 °C/min in N_2 .

3. Results

3.1. ^{51}V NMR. For all of the samples, the ^{51}V MAS spectra consisted of superimposed patterns of spinning sidebands representing up to five sites (V_i , $i = 1, 2, \dots, 5$). We have conclusively shown in an earlier study³² that the vanadium species were predominantly in the V^{5+} oxidation state, and while the presence of a small concentration (no more than few percent) of paramagnetic V^{4+} species was possible, the discussion of the solid-state NMR data was relevant to most of the vanadium sites present in our gels. The previously proposed and discussed³² coordination for these sites has been illustrated in Figure 1. After publishing this earlier work, we have recognized an inconsistency in the convention used for reporting the simulated CSA tensor parameters for these vanadium sites. Thus, we reproduce in Table 1 the list of corrected line-shape parameters and give their proper definitions. We note that the quadrupolar parameters, the isotropic values of chemical shift, and, most importantly, the proposed spectral assignments were not affected by the aforementioned discrepancy.

The resonances present in sample I (Figure 2a) were consistent with our earlier results. However, the changes in the synthesis procedure used for this sample (as compared to our previous studies) resulted in some differences in the site

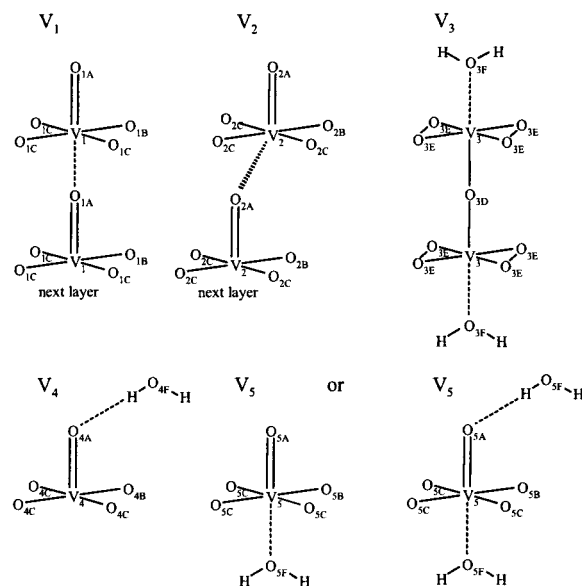


Figure 1. Proposed coordination of vanadia sites.³² The corresponding oxygen sites will be discussed later in the text.

Table 1. Isotropic Chemical Shifts (δ_{iso} in ppm), Spectral Linewidth (L_{CSA} in ppm), Chemical Shift Anisotropy ($\Delta\delta_{CSA}$ in ppm), and Asymmetry Parameter (η_{CSA}) of Various V_i Species Obtained by Numerical Simulations of ^{51}V MAS NMR Spectra Following the Thermal Treatment (Temperature T in °C)^{32a}

site	T	δ_{iso}	L_{CSA}	$\Delta\delta_{CSA}$	η_{CSA}	δ_{11}	δ_{22}	δ_{33}
V_1	25–100	–622.5	862	–741	0.49	–254	–497	–1116
	215	–618.5	917	–784	0.51	–224	–490	–1141
	224	–618.9	917	–784	0.51	–224	–491	–1141
	272	–619.4	920	–920	0.00	–313	–313	–1233
$V_2 + V_4$	550	–619.4	960	–960	0.00	–299	–299	–1259
	25–100	–593.2	1180	–978	0.62	–65	–469	–1245
	215	–592.6	1000	–909	0.30	–199	–380	–1199
	224	–594.6	887	–845	0.15	–271	–355	–1158
V_3	272	–597.2	1583	–1246	0.81	155	–518	–1428
	100	–663.6	1096	–931	0.53	–189	–518	–1285
	V_5	100	–572.3	1069	–1021	0.14	–184	–280

^a Values of $\Delta\delta_{CSA}$, η_{CSA} , and components of the CSA tensor (δ_{ii} in ppm, where $ii = 11, 22, 33$) are given using the following convention: $\delta_{iso} = (\delta_{11} + \delta_{22} + \delta_{33})/3$, $L_{CSA} = |\delta_{11} - \delta_{33}|$, $\Delta\delta_{CSA} = 3/2(\delta_{33} - \delta_{iso})$ and $\eta_{CSA} = (\delta_{22} - \delta_{11})/(\delta_{33} - \delta_{iso})$, assuming $|\delta_{33} - \delta_{iso}| \geq |\delta_{11} - \delta_{iso}| \geq |\delta_{22} - \delta_{iso}|$.

distribution as a function of temperature. The concentrations of various V_i sites based on simulations of the ^{51}V MAS spectra using QUASAR and the number of water molecules (n) per V_2O_5 based on the TGA data are given in Table 2. ^{51}V NMR resonances at –580, –593, –620, and –663 ppm were observed at 25 °C (see Figure 2a), which were previously assigned to V_5 , V_4 , V_1 , and V_3 sites, respectively.³² Following the thermal treatment to 224 °C, the resonance corresponding to the V_3 site vanished, while an additional resonance, ascribed to the V_2 site, was observed at –597 ppm (Figure 2a).³² Although the V_2 and V_4 sites could not be resolved by ^{51}V NMR, strong evidence has been previously provided for the presence of two resonances in the same spectral region (only one of which, V_4 , was coordinated with water).³² The ^{51}V NMR spectra obtained after heating to 272 and 325 °C contained resonances at –580, –597, and –620 ppm, corresponding to V_5 , $V_4 + V_2$ (predominantly V_2), and V_1 sites, respectively (Figure 2a). Following thermal treatment to 350 °C, only one resonance at –620 ppm remained, which represented the V_1 site in crystalline V_2O_5 .

(33) Kunwar, A. C.; Turner, G. L.; Oldfield, E. *J. Magn. Reson.* **1986**, *69*, 124.

(34) Amoureux, J.-P.; Fernandez, C.; Steuernagel, S. *J. Magn. Reson., Ser. A* **1996**, *123*, 116.

(35) Amoureux, P.; Fernandez, C.; Dumazy, Y. Abstract No. 264, 37th Rocky Mountain Conference, Denver, 1995.

(36) Amoureux, J.-P.; Fernandez, C. *Solid State Nucl. Magn. Reson.* **1998**, *10*, 211; **2000**, *16*, 339.

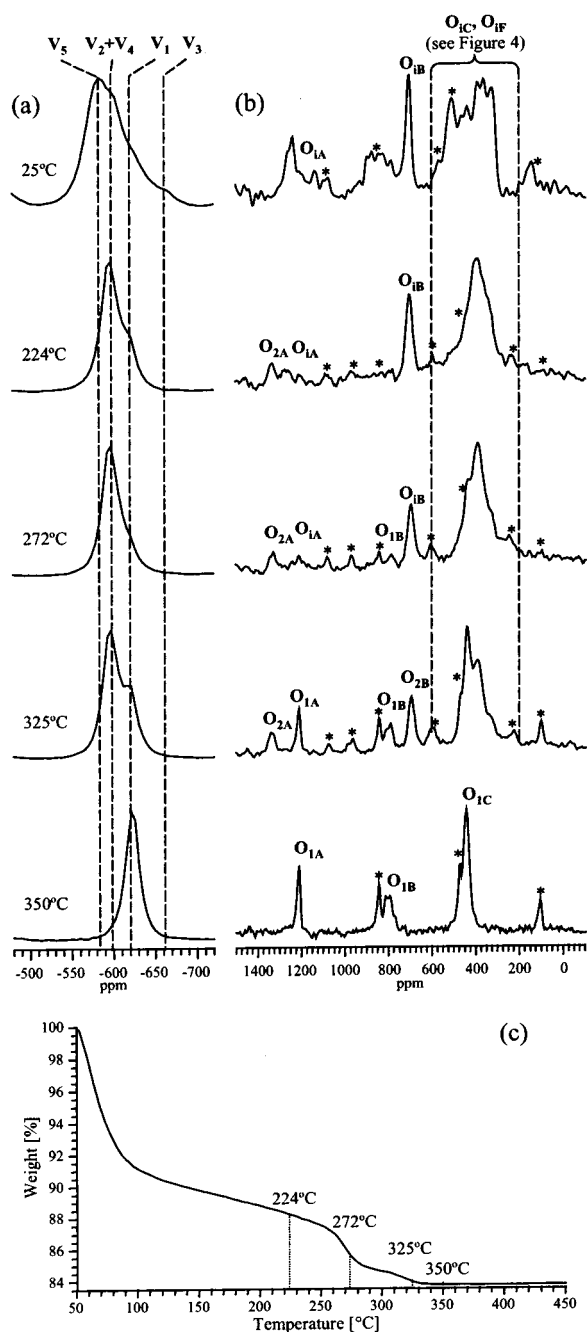


Figure 2. Analysis of sample **I**: (a) ^{51}V MAS NMR spectra, (b) ^{17}O MAS NMR spectra, and (c) the corresponding TGA weight loss curve. Asterisks denote the spinning sidebands.

Prior to rehydration of sample **II**, the ^{51}V NMR spectra (not shown) and TGA analysis (Figure 3c, solid line) were the same as reported earlier.³² Because no rehydration was observed in the case of crystalline V_2O_5 (i.e., sample treated at 350 °C), the sample used in this study was rehydrated after the initial thermal treatment to a lower temperature of 224 °C. However, even in this case, the rehydration was not reversible in the sense that it resulted in a different distribution of sites and a different response to further thermal treatment, see Figure 3a,c and Table 2. TGA of samples **I** and **II** in their as-prepared state indicated approximately 16 and 19 wt % water, corresponding to $n = 2$ and 2.4, respectively. Only one-half of that amount (corresponding to $n = 1$) was found in sample **II** after rehydration

Table 2. Number (n) of Coordinated H_2O Molecules per V_2O_5 and Relative Concentrations of Various V_i Species (in %) in the Vanadia Gels Obtained from Thermogravimetric Analysis and by Numerical Simulations of ^{51}V MAS NMR Spectra, Respectively

temp (°C)	n	V_1	V_2+V_4	V_3	V_5
sample I					
25	2.00	13	45 ^a	6	36
224	0.50	13	79		8
272	0.26	22	74		4
325	0.03	29	71 ^b		
350	0.00	100			
sample II as-synthesized ^c					
25	2.40	18	45 ^a	5	32
224	0.06	35	63		2
sample II rehydrated					
25	1.00	32	19 ^a	8	41
150	0.12	21	67	2	10
224	0.06	26	67		7
272	0.02	65	34 ^b		1
350	0.00	100			

^a V_4 only. ^b V_2 only. ^c Data were taken from ref 32.

(Figure 3c, dashed line). The TGA results were consistent with the ^{51}V MAS NMR spectra (Figure 3a) and indicated that the V_1 sites did not rehydrate (Table 2). Clearly, water preferably reabsorbed in the position trans to the vanadyl oxygen, forming site V_5 . Again, in agreement with the previous work, the concentration of this site decreased first, although in the rehydrated sample it declined at temperatures lower than 150 °C. As expected, the V_3 , V_4 , V_5 , and, last, V_2 sites gradually transformed to V_1 sites upon further heating to 350 °C, following the general scheme proposed in Figure 11 of ref 32. Note, however, that the concentration of V_1 sites in the rehydrated sample showed an initial decrease at 150 °C.

3.2. ^{17}O NMR. The ^{17}O NMR spectra consist of several groups of superimposed resonances, which include contributions from different sites, depending on the thermal treatment. To facilitate identification of the ^{17}O NMR assignments in this study, the oxygen sites have been labeled O_{ij} , where $i = 1, 2, \dots, 5$ denotes the corresponding vanadium site(s) (as discussed above), and $j = \text{A}, \text{B}, \dots, \text{F}$ indicates the type of oxygen site (A = singly coordinated, B = doubly coordinated, C = triply coordinated, D and E being the linear bridging and η^2 -peroxo oxygen of the dimer, respectively, and F being the coordinated water, as shown in Figure 1). Nearly all of the assignments were made on the basis of the spectra of sample **I**; scrambling may have occurred during thermal treatment of sample **II**, so that only the low temperature (25 °C) spectrum was considered in interpreting the ^{17}O lines. At least 13 different oxygen resonances were observed including the oxygen of chemisorbed water. The spectral assignments will be described in detail in the Discussion section. A short summary of the assignments and the approximate values for the observed shifts have been provided in Table 3.

Oxygen sites were distinguished using ^{17}O MAS (Figures 2b and 3b) and 3QMAS (Figures 4 and 5) NMR. The ^{17}O MAS NMR spectra consisted of superimposed patterns of spinning sidebands representing several oxygen sites with a wide variety of CSA powder patterns. The center bands for the different sites were present in three general regions: 1400–1100, 850–700, and 600–200 ppm. This is in agreement with a previous ^{17}O NMR HETCOR study of the decavanadate anion in solution³⁷ and ^{17}O MAS NMR investigation of a chain-structured vanadia

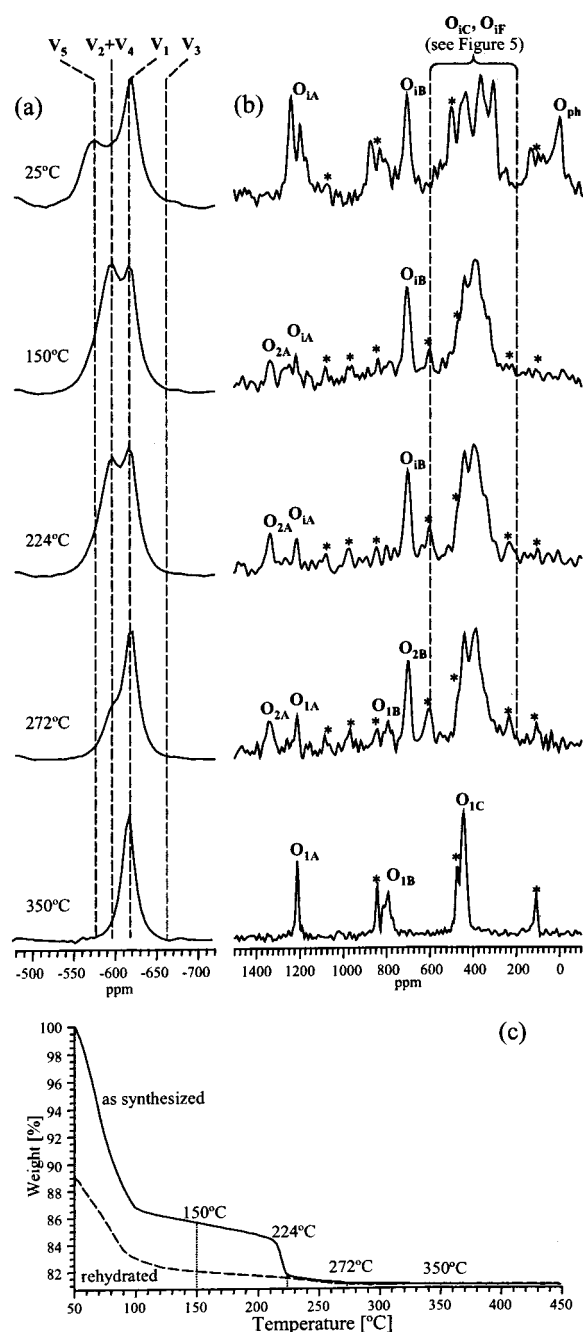


Figure 3. Analysis of sample **II** after rehydration: (a) ^{51}V MAS NMR spectra, (b) ^{17}O MAS NMR spectra, and (c) the corresponding TGA weight loss curve. TGA curve for as-synthesized sample **II** is also shown (solid line). Asterisks denote the spinning sidebands, while O_{ph} indicates physisorbed water.

gel,¹² which indicated that the vanadyl, doubly coordinated, and triply coordinated oxygen resonances for those materials were observed in the 1450–1050, 850–670, and 500–200 ppm regions, respectively.

MQMAS experiments do not generally yield reliable quantitative information because changes in the quadrupolar coupling constant C_Q , the asymmetry parameter η_Q , and CSA can affect the efficiency of multiple quantum transfers. In the 3QMAS experiments reported here, only resonances between 600 and 200 ppm were detectable. Most likely, the spectral region

Table 3. Average Values of Isotropic Chemical Shifts (δ_{iso}) and Second-Order Quadrupolar Effect Parameters (P_Q) Determined from ^{17}O 3QMAS or MAS NMR Spectra for the Oxygen Sites Found in Samples **I** and **II** during Thermal Treatment between 25 and 325 °C^a

site	δ_{iso} (ppm)	P_Q (MHz)	method
$\text{O}_{5\text{F}}$	330	3.2	3QMAS
$\text{O}_{445\text{F}}$	375	3.1	3QMAS
$\text{O}_{2\text{C}} \text{O}_{4\text{C}} \text{O}_{5\text{C}}$	400–420	3.2	3QMAS
$\text{O}_{1\text{C}}$	465	3.7	3QMAS
$\text{O}_{4\text{F}}$	510	4.4	3QMAS
?	600	4.8	3QMAS
$\text{O}_{2\text{B}} \text{O}_{4\text{B}} \text{O}_{5\text{B}}$	700		MAS
$\text{O}_{1\text{B}}$	820		MAS
$\text{O}_{3\text{D}}$	1135		MAS
$\text{O}_{4\text{A}}$	1170		MAS
$\text{O}_{1\text{A}}$	1210		MAS
$\text{O}_{5\text{A}}$	1240		MAS
$\text{O}_{2\text{A}}$	1330		MAS

^a The data were obtained with the average accuracies of ± 10 ppm and ± 0.3 MHz for δ_{iso} and P_Q , respectively.

between 1400 and 1100 ppm is unobservable by this method because of small C_Q values and large CSA for the vanadyl sites, whereas resonances for the doubly coordinated oxygen sites expected between 850 and 700 ppm were probably not detected because of large CSA. The C_Q and CSA values obtained for these sites from the simulation of the ^{17}O MAS spectrum of crystalline V_2O_5 were consistent with this explanation, as indicated in Table 4 (sites $\text{O}_{1\text{A}}$ and $\text{O}_{1\text{B}}$). For the sites that were observed by the MQMAS method, the values for the so-called second-order quadrupolar effect parameter $P_Q = C_Q(1 + \eta_Q^2/3)^{1/2}$, as determined from the spectra, were between 2.5 and 4.8 MHz. Assuming no large changes in the CSA, we found that the relative 3QMAS efficiencies for these sites can vary by as much as 50% for the experimental conditions used in our work.

3.2.1. Sample I. For the as-synthesized sample **I**, several oxygen resonances were observed in the vanadyl region of the MAS spectrum between 1250 and 1120 ppm, which were labeled $\text{O}_{i\text{A}}$ in the top trace of Figure 2b. The deconvolution of this part of the spectrum (and the corresponding trace for sample **II**) pointed to the presence of three resonances at 1240 ($\text{O}_{5\text{A}}$), 1210 ($\text{O}_{1\text{A}}$), and 1170 ppm ($\text{O}_{4\text{A}}$). An additional small peak was detected at 1135 ppm ($\text{O}_{3\text{D}}$). Other resonances were observed at around 700 ppm ($\text{O}_{i\text{B}}$, $i = 4$ and 5) and in the 600–200 ppm range. The number of sites contributing to the spectrum between 600 and 200 ppm (labeled $\text{O}_{i\text{C}}$ and $\text{O}_{i\text{F}}$) could not be determined from the MAS spectrum alone, as it contained a number of superimposed powder patterns representing the central transition of several resonances. Surprisingly, the 3QMAS method revealed a minimum of five resonances in this region at 25 °C (see the isotropic dimension in the spectrum of Figure 4 and Table 3). The isotropic chemical shifts corresponding to these sites were 330 ($\text{O}_{5\text{F}}$), 375 ($\text{O}_{445\text{F}}$), 410 ($\text{O}_{4\text{C}}$ and $\text{O}_{5\text{C}}$), 465 ($\text{O}_{1\text{C}}$), and 510 ppm ($\text{O}_{4\text{F}}$). No changes were observed in the MAS or 3QMAS spectra following heating of sample **I** to 100 °C (spectra not shown). However, after heating to 224 °C, the changes had occurred in the general line shape of the vanadyl region, and a new peak $\text{O}_{2\text{A}}$ was observed around 1330 ppm (Figure 2b). Resonances at 1250–1120, 700, and 600–200 ppm were still present. The corresponding 3QMAS spectrum revealed that the peaks at 330 and 375 ppm had decreased in intensity (see Figure 4). After thermal treatment to 272 °C, vanadyl resonances $\text{O}_{i\text{A}}$ weakened, whereas those at 1330, 700, and 600–200 ppm

(37) Wagner, G. W. *Inorg. Chem.* **1991**, *30*, 1960.

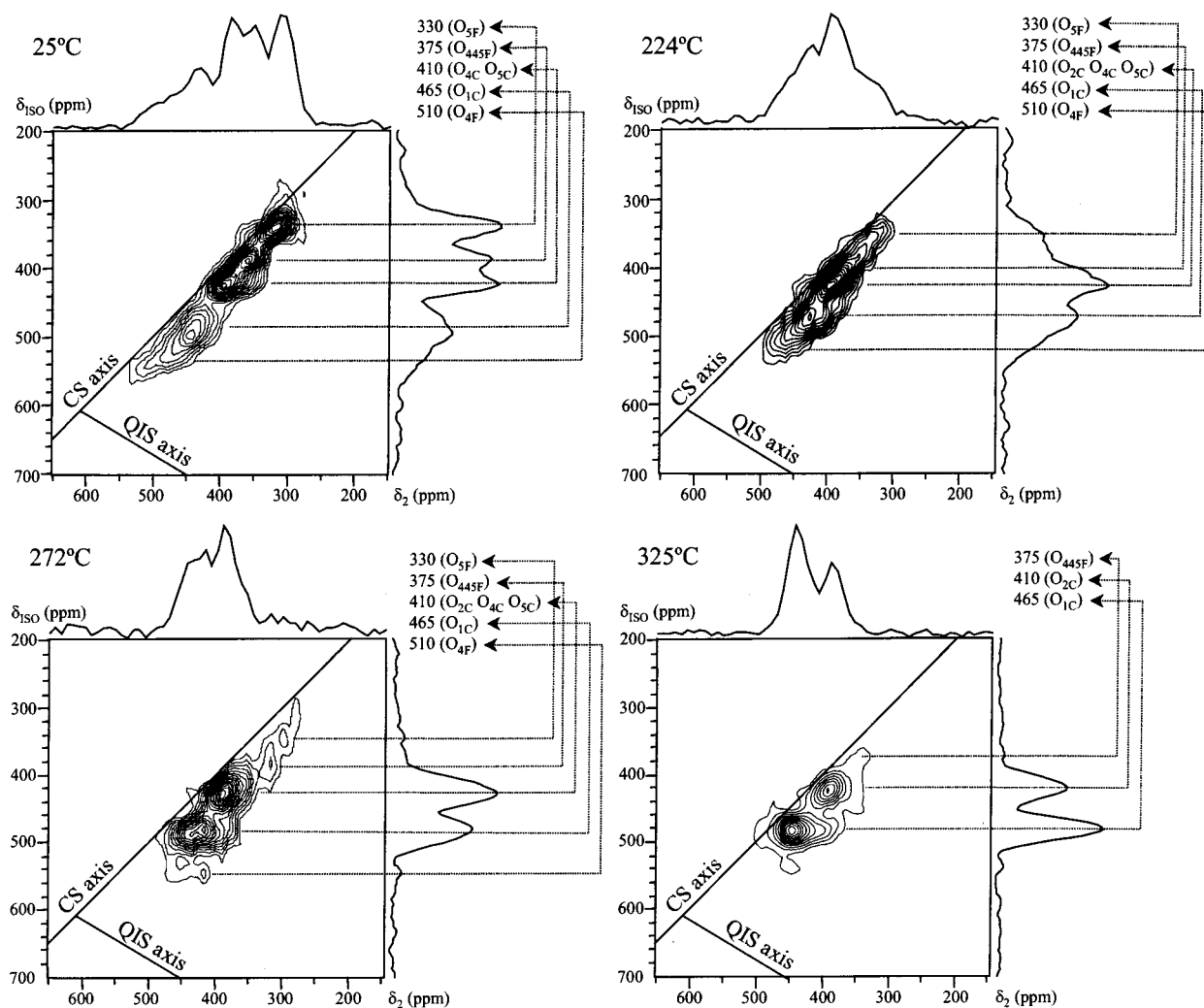


Figure 4. Sheared ^{17}O 3QMAS spectra of sample **I** at 25, 224, 272, and 325 °C. The isotropic (vertical) and anisotropic (horizontal) dimensions are labeled following the convention described in ref 36. The isotropic chemical shifts for various oxygens sites were determined by projecting the center of gravity of the corresponding lines on the chemical shift (CS) axis along the direction of the quadrupole-induced shift (QIS) axis.

remained quite strong. Another center band is visible at 820 ppm ($\text{O}_{1\text{B}}$), which could not be distinguished from noise and MAS sidebands at lower temperatures. Resonances were observed in the 3QMAS experiment at 330, 375, 410, 465, and 510 ppm, as labeled in Figure 4. After heating to 325 °C, we found that the resonances in the MAS spectrum were observed at 1330, 1210, 820, 700, and 600–200 ppm (Figure 2b). At this stage, the 3QMAS spectrum revealed that the spectral region between 600 and 200 ppm included strong peaks at 465 ($\text{O}_{1\text{C}}$) and 410 ppm (predominantly $\text{O}_{2\text{C}}$) along with a weak resonance at 375 ppm ($\text{O}_{445\text{F}}$) (Figure 4). Following heating to 350 °C, we found that a crystalline structure emerged and the MAS spectrum contained resonances at 1213 ($\text{O}_{1\text{A}}$), 824 ($\text{O}_{1\text{B}}$), and 474 ppm ($\text{O}_{1\text{C}}$) (see bottom trace of Figure 2b, Figure 6d, and Table 4). This MAS spectrum allowed for full line-shape analysis, and thus the MQMAS experiment has not been performed for this temperature. After heating to 550 °C, we found that the same resonances were observed (spectrum not shown), although the fwhm of each peak had decreased, which was consistent with progressing crystallization. During the dehydration process, the line shape corresponding to the vanadyl region of the ^{17}O MAS spectra changed (Figure 2b) noticeably. This is consistent with our previously reported ^{51}V MAS NMR

study, which indicated that the line-shape parameters of the corresponding vanadia sites had also changed upon the removal of water.³²

3.2.2. Sample II. The ^{17}O MAS and 3QMAS NMR spectra of rehydrated sample **II** were surprisingly similar to the corresponding spectra of sample **I** (compare Figures 2b and 3b and Figures 4 and 5). The main differences involved the signal at 375 ppm ($\text{O}_{445\text{F}}$) (less intense in the 3QMAS spectrum of sample **II**), the signal at 600 ppm (only observed in the 3QMAS spectrum of sample **II** at low temperatures), the signal at 1135 ppm ($\text{O}_{3\text{D}}$) (not observed in the spectra of sample **II**), and the signal at around 0 ppm in sample **II** representing physisorbed water. The similarity of these results indicated that (i) incorporation of ^{17}O nuclei from H_2^{17}O took place under the mild conditions used during rehydration, and (ii) oxygen had exchanged rather uniformly in the gel.

4. Discussion

4.1. Structure of Crystalline and Layered Samples at Various Stages of Dehydration. Previous reports have indicated that the amorphous vanadia gels crystallize into orthorhombic V_2O_5 following thermal treatment at 350 °C.³⁸ Our assignments

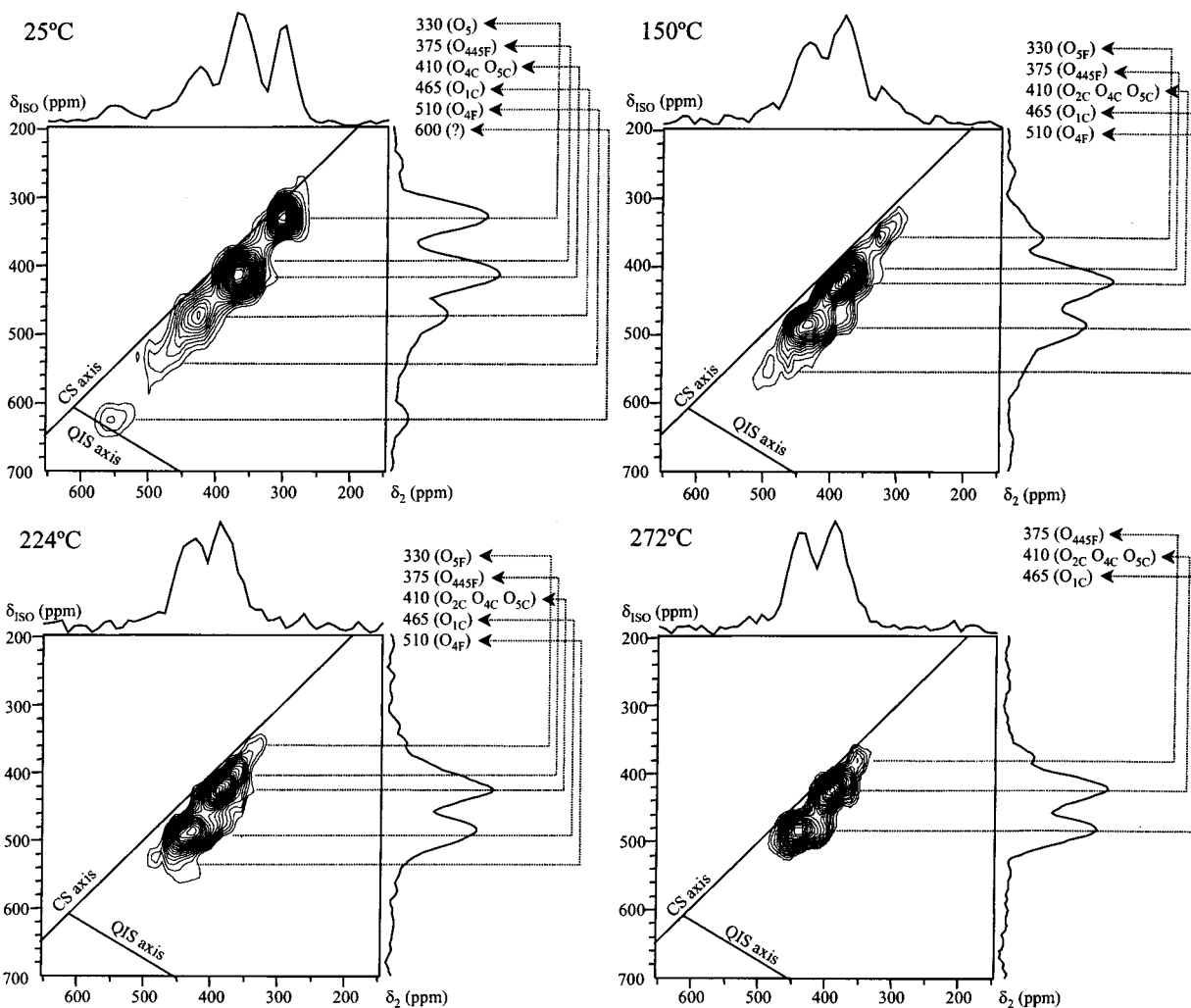


Figure 5. Sheared ^{17}O 3QMAS spectra of sample **II** at 25, 150, 224, and 272 $^{\circ}\text{C}$. The spectra were processed as described in the caption of Figure 4.

Table 4. Results of Numerical Simulation of ^{51}V and ^{17}O MAS Spectra of Crystalline V_2O_5 , Formed after Thermal Treatment of Sample **I** at 350 $^{\circ}\text{C}$ ^a

site	δ_{iso}	$\Delta\delta_{\text{CSA}}^b$	η_{CSA}	C_Q	η_Q
V_1	-620	-940	0.2	0.9	0.1
$\text{O}_{1\text{A}}$	1213	2000	1.0	0.9	0.6
$\text{O}_{1\text{B}}$	824	400	0.4	4.0	0.7
$\text{O}_{1\text{C}}$	474	0	0.0	3.3	0.6

^a The data were obtained with the following accuracy: C_Q , ± 0.1 MHz; η_Q and η_{CSA} , ± 0.1 ; δ_{iso} , ± 1 ppm; $\Delta\delta_{\text{CSA}}$, ± 50 ppm. ^b For definition, see Table 1.

and discussion focus first on this material because its structure is well understood.

4.1.1. 350 $^{\circ}\text{C}$. The XRD studies indicated that only one type of vanadium site (V_1) and three different oxygen sites exist in crystalline V_2O_5 , as shown in Figure 6a,b.³⁹ The ^{51}V MAS spectrum of sample **I** treated at 350 $^{\circ}\text{C}$, which is shown in Figure 2a (bottom trace) and expanded in Figure 6c, was consistent with this structure. The simulation of this spectrum (Table 4) yielded line-shape parameters similar to those published earlier (Table 1 and refs 40–44). The corresponding ^{17}O MAS NMR

data (Figure 6d) clearly revealed three distinct resonances with the corresponding isotropic chemical shifts of 1213, 824, and 474 ppm (Table 4). On the basis of the liquid-state NMR studies of similar oxygen environments,³⁷ these resonances have been assigned to the vanadyl oxygen ($\text{O}_{1\text{A}}$), the doubly coordinated oxygen ($\text{O}_{1\text{B}}$), and the triply coordinated oxygen ($\text{O}_{1\text{C}}$), respectively, as shown in Figure 6a,b. For the vanadyl and doubly coordinated oxygen sites, our assignments are similar to those made by McCormick et al. in a solid-state NMR study of a chain-structured vanadia gel.¹² However, McCormick et al. did not observe any triply coordinated oxygen sites. The large CSA value for the vanadyl oxygen ($\text{O}_{1\text{A}}$) obtained via the simulations of the ^{17}O MAS spectrum (Table 4) was consistent with other studies of organic doubly bonded oxygen compounds.⁴⁵ The C_Q values calculated for each oxygen site were found to be in the order $\text{O}_{1\text{B}} > \text{O}_{1\text{C}} > \text{O}_{1\text{A}}$. This trend was consistent with the calculated populations of the p_z orbitals [perpendicular to the (001) plane] of these nuclei in crystalline V_2O_5 .⁴⁶

(38) Aldebert, P.; Baffier, N.; Gharbi, N.; Livage, J. *Mater. Res. Bull.* **1981**, *16*, 669.

(39) Byström, A.; Wilhelmi, K. A.; Brotzen, O. *Acta Chem. Scand.* **1950**, *4*, 1119.

(40) Gornostansky, S. D.; Stager, C. V. *J. Chem. Phys.* **1967**, *46*, 4959.

(41) France, P. W. *J. Magn. Reson.* **1991**, *92*, 30.

(42) Skibsted, J.; Nielsen, N. C.; Bildsøe, H.; Jakobsen, H. *J. Chem. Phys. Lett.* **1992**, *188*, 405.

(43) Fernandez, C.; Bodart, P.; Amoureux, J.-P. *Solid State Nucl. Magn. Reson.* **1994**, *3*, 79.

(44) Marichal, C.; Kempf, J.-Y.; Maigret, B.; Hirschinger, J. *Solid State Nucl. Magn. Reson.* **1997**, *8*, 33.

(45) Wu, G.; Dong, S. *Chem. Phys. Lett.* **2001**, *334*, 265.

(46) Witko, M.; Tokarz, R.; Haber, J. *J. Mol. Catal.* **1991**, *66*, 205.

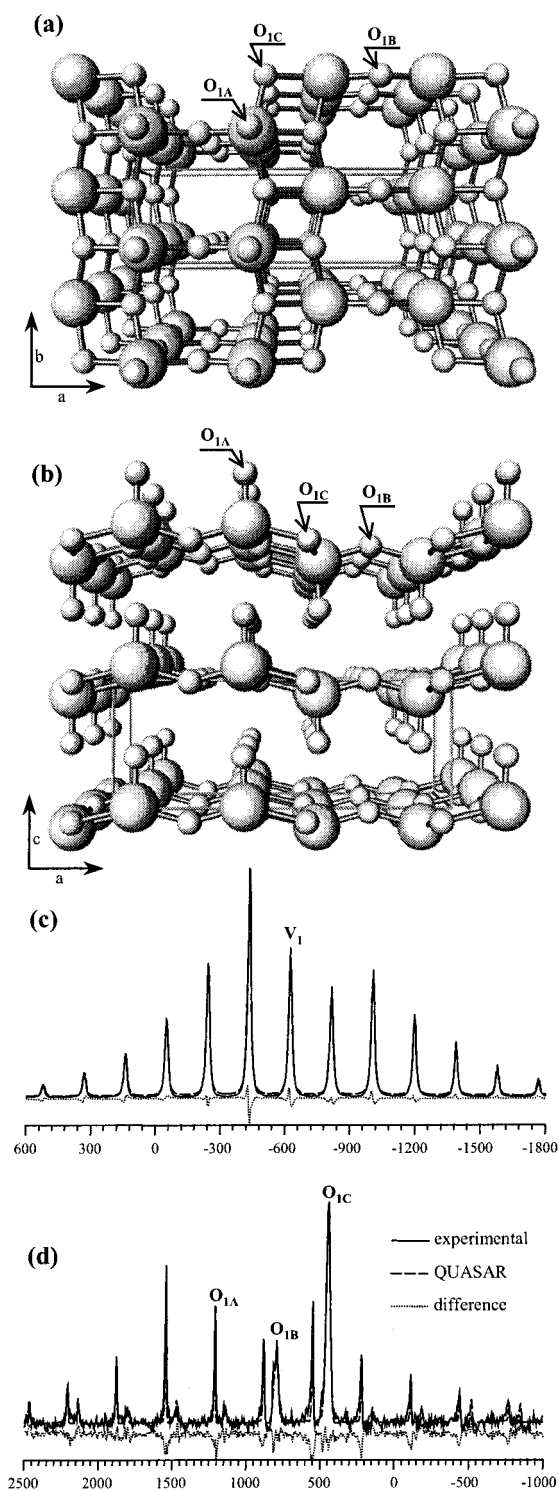


Figure 6. Crystalline V_2O_5 : (a) 001 plane and (b) 010 plane obtained from the XRD studies;³⁹ (c) and (d) extended sideband pattern of ^{51}V MAS and ^{17}O MAS NMR spectra of sample **I** after thermal treatment to 350 °C, measured using rotation rates of 20 and 18 kHz, respectively. The corresponding simulations of NMR line shapes are shown, as well.

4.1.2. 325 °C. The ^{17}O MAS and 3QMAS NMR spectra of sample **I** after thermal treatment to 325 °C (Figures 2b and 4) revealed three additional resonances at 1330, 700, and 410 ppm. Because two vanadium sites V_1 and V_2 dominated the ^{51}V spectrum of this sample (Figure 2a and Table 2), these signals were assigned to the vanadyl (O_{2A}), the doubly coordinated

(O_{2B}), and the triply coordinated (O_{2C}) species of the V_2 site. Note that the O_{2A} species was not detected at 25 °C (the lack of sites O_{2B} and O_{2C} could not be clearly established because of overlap with other resonances), which was in agreement with our previous hypothesis that V_2 sites were not present in as-prepared samples but were created at the expense of V_3 , V_4 , and V_5 sites as the water molecules were released.³² The presence of V_2 sites was consistent with the model of the layered gel structure in which the adjacent planes were shifted in the ab plane.^{32,47} The detection of the corresponding O_{2j} sites further validates this model (see section 4.1.5.).

Also note here that the strong resonance at around 700 ppm in the ^{17}O MAS spectrum (labeled O_{1B} in Figure 2b) persisted at all temperatures below 325 °C. At 325 °C, it was just assigned to O_{2B} , a site that does not exist at 25 °C. The presence of this peak at 25 °C can be reasonably explained by assigning it to similar types of oxygen sites, specifically O_{4B} and O_{5B} . The observed downfield shift of this resonance from 704 to 696 ppm with progressing dehydration reinforces the idea that it represents more than one species. A similar argument can be made for the resonance at around 410 ppm, which shifted between 400 and 420 ppm during dehydration (labeled O_{1C} in Figure 2b). Most likely, this resonance corresponded to O_{2C} at 325 °C, O_{4C} and O_{5C} at 25 °C, and a mixture of all three species (O_{2C} , O_{4C} , and O_{5C}) at the intermediate stages of hydration.

4.1.3. 272 °C. Another weak resonance, at about 375 ppm, was identified in the 3QMAS spectra of sample **I** at 272 °C (Figure 4). We previously proposed that water remaining at this stage of hydration was shared between two V_4 sites and a V_5 site.³² Therefore, the ^{17}O resonance at 375 ppm was assigned to this species and was labeled O_{445F} . A residual amount of this species may still be observed under 3QMAS at 325 °C. Even at room temperature, this resonance was strong in sample **I** (Figure 4), indicating that this type of coordination was prevalent in the as-prepared gel. To accommodate this site, the adjacent layers would have to shift slightly in the ab plane, which further supports our interpretation of the observed V_2 and O_{2j} sites (again, see section 4.1.5.).

4.1.4. 25–224 °C. Following heating of sample **I** between 25 and 224 °C, we found that the most significant changes in the ^{51}V NMR spectra (Figure 2a) involved the V_3 and V_5 sites. The relative concentrations of these sites decreased from 6 to 0% and 36 to 8%, respectively (Table 2). Comparison of the ^{17}O 3QMAS spectra (Figure 4) obtained in this temperature range indicated that the strong resonances at 330 and 375 ppm (and weaker lines at 345, 475, and 510 ppm) had decreased, as well, with increasing temperature. The resonance at 375 ppm was already assigned to shared water, O_{445F} . The resonance at 330 ppm was most easily assigned by examining the rehydrated gel. The ^{51}V NMR spectrum of sample **II** at 25 °C (Figure 3a) indicated that, except for V_1 , the most prevalent vanadium site was V_5 . The corresponding 3QMAS spectrum (Figure 5) revealed that the resonance at 330 ppm was also dominant. Upon heating of sample **II** to 70 °C (spectra not shown), we found that both the V_5 site concentration and the intensity of the ^{17}O resonance at 330 ppm decreased. This strongly suggested that it corresponded to water coordinated at the V_5 site (O_{5F}). There

(47) Hibino, M.; Ugaji, M.; Kishimoto, A.; Kudo, T. *Solid State Ionics* **1995**, *79*, 239.

was no spectroscopic evidence that this water was shared with any other vanadium site.

The assignment of the remaining, weak resonance at 510 ppm in the 3QMAS spectra is uncertain. Because this resonance was still present after V_3 had disappeared (at 224 °C) and the oxygen sites associated with V_5 have been rather unambiguously assigned, association with those sites is unlikely. The presence of this resonance coincided with the presence of the V_4 sites so a plausible explanation could involve water coordinated to a single V_4 site (O_{4F}). Peaks present in the vanadyl oxygen region of 1250–1120 ppm are not completely resolved, and their assignment is somewhat equivocal, as well. However, by correlating the intensities of deconvoluted resonances at 1240, 1210, 1170, and 1135 ppm (in samples **I** and **II**) with the corresponding intensities from sites V_1 , $V_2 + V_4$, V_3 , and V_5 , these resonances could be assigned to O_{5A} , O_{1A} (site assigned earlier), O_{4A} , and O_{3D} (for this site, see next paragraph), respectively.

Finally, we have earlier postulated that a small concentration (~5%) of V_3 sites found in the ^{51}V spectra of fully hydrated samples represented a dimer structure.³² If this assignment of the V_3 site was correct, three additional weak resonances O_{3D} , O_{3E} , and O_{3F} would be expected at approximately 1100, 450, and 350 ppm.^{12,48,49} However, because of the complexity of the ^{17}O spectra, conclusive evidence for the presence of such sites could not be provided, with the exception of the O_{3D} site observed in the spectra of as-synthesized sample **I** at 1135 ppm.

We note that the ^{17}O signals for water coordinated to V^{5+} oxide species in solution were previously reported⁴⁹ in the 100–0 ppm region, while the signal for a triply coordinated water in the chain-structured vanadia gel was reported at 220 ppm.¹² The triply coordinated oxygen species present in decavanadate anions have been reported at about 440 ppm.³⁷ The signals for all of the coordinated water in our gels fell within the 600–200 ppm region, which seemed consistent with triply coordinated oxygen. Thus, it seems likely that the oxygen atom (O_{4F}) of the water molecule of the V_4 site was triply coordinated as well, and most likely hydrogen bonded to another water molecule. One example of such a hydrogen-bonded structure was proposed by Vandendorre et al.,²² where one OH bond of water was in the same direction as the $V=O$ bond.

The general types of water coordination proposed for the gel studied in this work are consistent with those predicted in the computational studies by Yin et al. of adsorbed water onto the most thermodynamically stable (010) plane of crystalline V_2O_5 .²⁷ These simulations indicated two preferential adsorption sites for water: (1) water hydrogen bonded to two adjacent vanadyl oxygens and (2) water coordinated directly to a vanadium atom. Similarly, computational studies of the (001) plane of crystalline V_2O_5 reported by Ranea et al. concluded that the preferred site for water chemisorption involved the vanadyl oxygen.²⁶ The additional water coordination sites that we have proposed for our multilayered gels include a water molecule shared between two V_4 sites and a V_5 site, a water molecule shared between one V_4 site and a V_5 site, and a water molecule associated with a dimer (V_3). Clearly, the gel layers cannot be considered as exposed surfaces, and the adsorption sites may be expected to differ from those found in crystalline V_2O_5 .

4.1.5. Layered Structure of $V_2O_5 \cdot nH_2O$ Gels. In our earlier study, we have used powder X-ray diffraction to show that our layered gels in their as-synthesized state (which corresponded to $n \cong 2.4$) consisted of repeating units with an interlayer distance c of approximately 13 Å.³² It was not clear, however, if this spacing corresponded to the adjacent layers, or if a second set is interleaved between these layers in incommensurate positions, as proposed earlier in the XRD study by Hibino et al.⁴⁷ According to Hibino's model, the layers are parallel and equidistant, with the middle layer being translated to some extent in the ab plane. Other reports (see the Introduction) of $c = 11.55$ Å for $n = 1.6$ and $c = 8.75$ Å in case of $n = 0.5$ – 0.6 ,^{21,23–25} while consistent with our XRD data, did not imply the presence of an additional interlayer and, consequently, proposed different coordination of water in the gels. After complete dehydration, the crystalline structure of V_2O_5 is known to have the lattice constant of 4.37 Å.³⁹ Because we have noticed only a moderate (~30–40%) volume reduction of sample **I** during the dehydration process, this large reduction of the c value is consistent with the proposed transition from a misaligned layer structure with the interlayer spacing of $1/2 \cdot 11.55$ Å $\cong 5.8$ Å into a fully aligned, crystalline structure with $c = 4.37$ Å.

Our ^{51}V and ^{17}O NMR results strongly validate the presence of a shifted layer. As was already pointed out in section 4.1.2., the presence of two sets of ^{51}V and ^{17}O resonances in the sample treated at 325 °C is fully consistent with this model. Upon complete removal of water at 350 °C, we detected only one set of sites as the crystalline V_2O_5 structure was formed. In samples with higher water content, the O_{445F} sites were assigned to the water molecules that were trapped between the adjacent planes. Two such sites would be created by assuming a shift between these planes of approximately ± 1.7 Å along the a axis, as proposed in Figure 7. A smaller shift, of less than ± 0.5 Å, would be expected along the b axis to accommodate the bond between water and the V_5 site. Site **1** corresponds to a water molecule coordinated to a vanadium V_5 site and two vanadyl oxygen atoms O_{4A} . In site **2**, water is also coordinated to a V_5 site; however, only one hydrogen bond to site O_{4A} is possible, which makes such coordination energetically less favorable. The water molecule is located in such way that the V_5 – O_{445F} (V_5 – O_{5F}) distance is approximately 1.7 Å, while the O_{4A} – O_{445F} (O_{4A} – O_{5F}) distance is close to 2 Å in both sites. A similar layer adjustment (2.46 Å along the a axis and 0.25 Å along the b axis) was proposed in ref 47. Also note that the induced shift in the ab plane shortens the distance between vanadyl oxygen atoms located in two neighboring layers from 3.0 to 2.4 and 1.5 Å. This would allow a proton to easily jump between the vanadyl oxygen atoms and explain the high proton conductivity of vanadia gels.⁵⁰

4.2. Rehydration. The rehydration experiments involving $H_2^{17}O$ were initially undertaken with the intent of simplifying the assignments of the water adsorption sites. Thus, as-synthesized sample **II** was first dehydrated at 224 °C, the temperature at which only 0.06 water molecule per V_2O_5 was left, and yet there was about 60% of V_2 sites present (Table 2),³² and then cooled to room temperature and placed in ^{17}O -enriched water vapor. The discovery that oxygen had exchanged under such mild conditions from adsorbed water to the oxygen sites in the gel was quite surprising, especially because an

(48) Reynolds, M. S.; Butler, A. *Inorg. Chem.* **1996**, *35*, 2378.

(49) Harrison, A. T.; Howarth, O. W. *J. Chem. Soc., Dalton Trans.* **1985**, 1173.

(50) Barbour, P.; Morineau, R.; Livage, J. *Solid State Ionics* **1988**, *27*, 221.

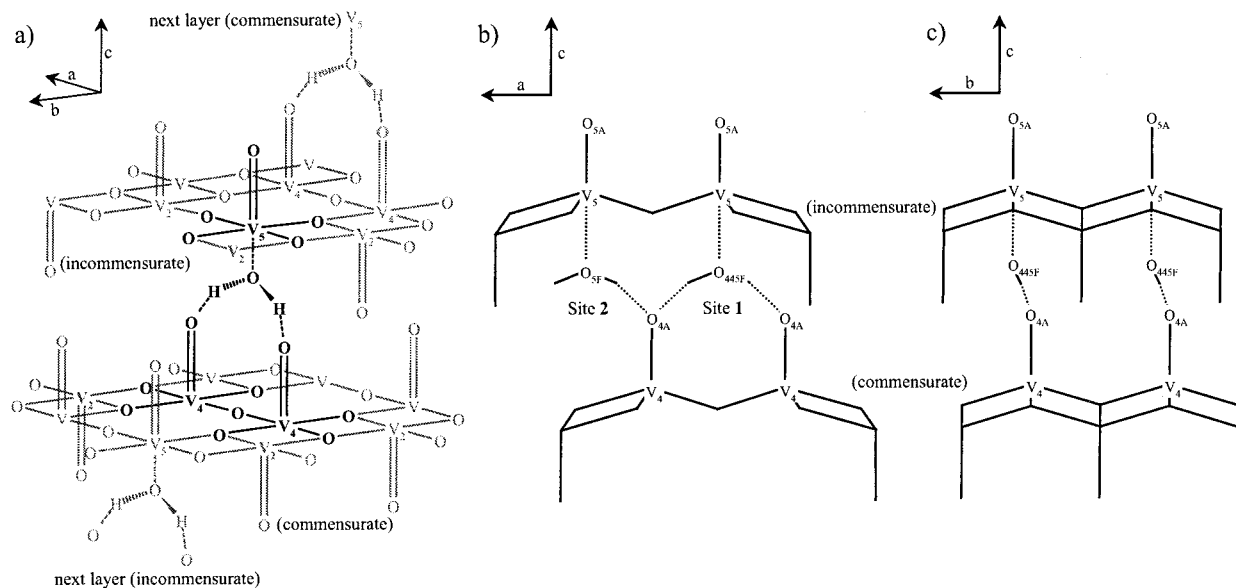


Figure 7. Proposed structure of a layered vanadium gel with the sites (V_4 and V_5) corresponding to the most strongly bound water (O_{445F} – site 1). Parts b and c were constructed from crystalline data³⁹ by shifting the top layer by 1.7 Å along the a axis and by 0.5 Å along the b axis, which created two possible sites for water adsorption. For clarity, only selected sites are marked.

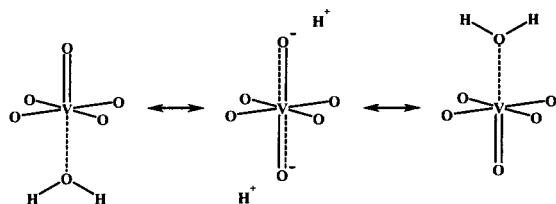
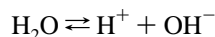


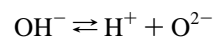
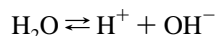
Figure 8. Postulated resonance structure involving water and the vanadyl oxygen.

exchange of the ^{18}O -form-enriched water into Alundum-supported V_2O_5 catalyst system required high temperatures.²⁸ Except for the absence of the signal at 375 ppm (O_{445F}) in sample **II**, the ^{17}O MAS and 3QMAS spectra for samples **I** and **II** were similar at every stage, indicating that ^{17}O had exchanged into all of the sites in the gel structure. The ^{51}V MAS NMR results of sample **II** at 25 °C showed that water preferentially readsorbed trans to the vanadyl oxygen, creating a V_5 site (Figure 3a, 25 °C). Because the V_1 sites are expected to be fairly stable, and no V_2 sites were present following rehydration (no O_{2A} sites were observed), it seems likely that the readsorbed water created a V_5 site by coordinating with a V_2 site. It is interesting that for the rehydrated gel, some of the water lost below 100 °C was chemisorbed (V_5 site). This was in contrast to sample **I**, where only the physisorbed water was lost below 100 °C.

Several possible exchange mechanisms in the vanadia gels may be considered. According to conductivity measurements,⁵⁰ the H^+ species in the layered gels are quite mobile. This would suggest a partial or complete dissociation process occurring with the adsorbed water. Partial dissociation



would yield OH^- and H^+ species. Complete dissociation



would produce O^{2-} and H^+ moieties. Considering the reactivity of the oxygen species (i.e., the relative ease of oxygen exchange), we expect that the O^{2-} species may be more likely. Because the O^{2-} species would be very unstable (and therefore reactive), its existence would probably depend on the presence of a catalyzed process or a resonance structure. The presence of a coordinated water molecule trans to the vanadyl oxygen could give rise to a short-lived resonance structure, such as the one depicted in Figure 8. Because the coordinated water (O_{5F}) in this structure was observed at about 330 ppm and the $\text{V}=\text{O}$ (O_{5A}) was thought to be observed at about 1240 ppm, a motinally averaged signal might be expected at about 700 ppm. The unassigned ^{17}O signal at approximately 600 ppm, which was observed only in sample **II** at 25 °C (and at 70 °C, not shown), may correspond to such a structure. These resonance stabilized oxygen atoms would conceivably be very reactive and might be expected to exchange into the gel oxygen sites.

The discovery that the oxygen of water exchanges so readily with the oxygen sites in the gel may indicate that these layered materials are suitable for very low-temperature oxidation catalysis, and work is currently underway in our laboratories to determine the catalytic properties of these materials. Using these ^{17}O -labeled catalysts, we believe it should now be possible to determine what oxygen site(s) are responsible for each insertion in the selectively oxidized products. Additional experiments are underway to examine the underlying fundamental phenomena (i.e., dissociation, competitive adsorption, changes in bond strength) which were found to result in improved activity and product selectivities observed following the addition of water to the feedstock.

Acknowledgment. This research was supported at Ames Laboratory by the U.S. Department of Energy, Office of Basic Energy Sciences, Division of Chemical Sciences, under contract W-7405-Eng-82. We also thank Prof. J. F. Stebbins for kindly providing the sample of ^{17}O -enriched silica.

JA0265254